

The effect of magnetic flutter on residual flow

P. W. Terry, M. J. Pueschel, D. Carmody, and W. M. Nevins

Citation: [Phys. Plasmas](#) **20**, 112502 (2013); doi: 10.1063/1.4828396

View online: <http://dx.doi.org/10.1063/1.4828396>

View Table of Contents: <http://pop.aip.org/resource/1/PHPAEN/v20/i11>

Published by the [AIP Publishing LLC](#).

Additional information on Phys. Plasmas

Journal Homepage: <http://pop.aip.org/>

Journal Information: http://pop.aip.org/about/about_the_journal

Top downloads: http://pop.aip.org/features/most_downloaded

Information for Authors: <http://pop.aip.org/authors>



Re-register for Table of Content Alerts

Create a profile.



Sign up today!



The effect of magnetic flutter on residual flow

P. W. Terry,¹ M. J. Pueschel,¹ D. Carmody,¹ and W. M. Nevins²

¹*Department of Physics, University of Wisconsin-Madison, Madison, Wisconsin 53706, USA*

²*Lawrence Livermore National Laboratory, Livermore, California 94551, USA*

(Received 11 September 2013; accepted 17 October 2013; published online 4 November 2013)

The hypothesis that stochastic magnetic fields disrupt zonal flows associated with ion temperature gradient turbulence saturation is investigated analytically with a residual flow calculation in the presence of magnetic flutter. The calculation starts from the time-asymptotic zero-beta residual flow of Rosenbluth and Hinton [Phys. Rev. Lett. **80**, 724 (1998)] with the sudden application of an externally imposed, fixed magnetic field perturbation. The short-time electron response from radial charge loss due to magnetic flutter is calculated from the appropriate gyrokinetic equation. The potential evolution has quadratic behavior, with a zero crossing at finite time. The crossing time and its parametric dependencies are compared with numerical results from a gyrokinetic simulation of residual flow in the presence of magnetic flutter. The numerical and analytical results are in good agreement and support the hypothesis that the high-beta runaway of numerical simulations is a result of the disabling of zonal flows by finite-beta charge losses associated with magnetic flutter.

© 2013 AIP Publishing LLC. [<http://dx.doi.org/10.1063/1.4828396>]

I. INTRODUCTION

For some time it has been known that numerical solution of comprehensive gyrokinetic models for ion temperature gradient (ITG) turbulence can encounter apparent difficulties in reaching a saturated steady state at finite beta.^{1,2} For the well known cyclone base case of ITG turbulence,³ the phenomenon arises for $\beta > 0.9\%$, a beta value for which ITG remains unstable, but is a significant fraction ($\sim 70\%$) of the critical beta for onset of the kinetic ballooning mode. While solutions of the linearized gyrokinetic equations yield a converged growth rate, nonlinear solutions, depending on initial conditions, can appear to reach a saturated state for short times, only to diverge away from this state with strongly growing amplitudes for later times. For this reason the phenomenon has been referred to as a runaway. Because it is observed with essentially identical features for a variety of gyrokinetic codes,⁴ it is not a pathology unique to any given code or numerical algorithm. While this alone does not rule out a numerical artifact as the source of the behavior, efforts to identify such an artifact have not been fruitful. On the other hand, several possible physical causes have been proposed.²⁻⁵

This paper deals with aspects of a proposed physical mechanism that has been successful in explaining critical features of the runaway phenomenon.⁵ The effect is rooted in the shorting of differences of zonal potential across rational surfaces by radial magnetic field perturbations arising at finite beta. The resulting elimination of zonal flows, given their association with significant reductions of transport in ITG turbulence, suggests that the runaway is not in reality a finite-beta regime of transport rates diverging toward infinity, but rather a regime of transport rates at finite but very high levels. Consequently, the phenomenon is better referred to as the non zonal transition (NZT), i.e., a transition at a critical beta to a turbulence regime of disabled zonal

flows and high transport. Large but saturated levels of turbulence and transport are in fact observed above the critical beta in simulation, as is the effective absence of zonal flows. The amplitudes are found to scale with gradients in a physically plausible way.⁵ Importantly, it has been demonstrated that the critical beta for the NZT to the large amplitude state is identical to the beta value required for irreversible electron motion along a radially perturbed field. It remains to understand (1) why a magnetic field capable of inducing irreversible behavior arises in ITG turbulence and (2) what such a magnetic field does to zonal flows in detail.

The first question has been answered in a series of nonlinear gyrokinetic simulations that show that ITG turbulence at beta values well below the NZT threshold of 0.9% nonlinearly excites stable modes with tearing parity, including a subdominant (stable) microtearing mode of sizable amplitude that produces a stochastic magnetic field and significant levels of electron thermal transport.^{6,7} An important aspect of the second question was addressed by examining the effect of a stochastic magnetic field on the residual flow.⁵ The residual flow is the time asymptotic plasma response to an impulsive perturbation of the zonal potential on a mode rational surface. While the impulsive perturbation is an artifact designed to expose underlying physics, it can be thought of as representing the near instantaneous charge configuration arising from mode coupling (over the short nonlinear correlation time). The impulsive response is only part of the physics that contributes to flow dynamics, but such a response can be created and isolated in simulation and compared with theory. The impulsive response in a toroidal plasma has been calculated in detail from neoclassical theory for zero beta.^{8,9} Comparisons with numerical calculations of the response from gyrokinetic and gyro Landau fluid codes were used to determine if flow responses are correctly handled in numerical algorithms at $\beta = 0$. When the response is correctly treated, an initial flow relaxes to a constant

residual flow on a timescale that is large relative to trapped particle bounce times, undergoing oscillations associated with geodesic acoustic modes along the way. The residual flow is governed by the radial excursions from rational surfaces of ions displaced by the grad-B and curvature drifts.

A perturbed magnetic field can affect the residual flow because electrons rapidly stream along the field. If they are unretrievably removed from the rational surface, the potential of that surface undergoes a change associated with the charge loss. The impulsive response and its residual flow asymptote have been calculated for the 3D helical magnetic field of a stellarator.^{10–12} Both the residual and the relaxation time differ from that of a tokamak. In some cases the temporal evolution goes monotonically from an initial value to a smaller residual of the same sign.^{10,11} In others, the zonal flow response is oscillatory.¹² Stellarator results are not generalizable to the tokamak in any straightforward way because they include the particle losses associated with 3D stellarator fields. A rough estimate of charge loss due to field stochasticity in a tokamak suggests that the charge on a rational surface will decay to zero and hence, too, the zonal flow. For example, consider an electrons-only calculation in which the equilibrium-field part of the parallel potential $\mathbf{B}_0 \cdot \nabla \phi / |B_0|$ is neglected to focus on the electron response to the potential by parallel motion along a radially perturbed field $\delta B_r = \nabla \psi \times \hat{\mathbf{z}}$. Then

$$m_e \frac{\partial}{\partial t} v_{\parallel} \sim e \nabla_{\parallel} \Phi = e \frac{\nabla \psi}{B_0} \times \hat{\mathbf{z}} \cdot \nabla \Phi = e \frac{\delta B_r}{B_0} E_r. \quad (1)$$

With flutter the temporal derivative is approximately given by the thermal velocity v_e divided by the magnetic correlation length l_m . The parallel velocity can thus be written

$$v_{\parallel} = \frac{e l_m}{m_e v_e} \frac{\delta B_r}{B_0} E_r. \quad (2)$$

Since $\delta J_r = -n_e e v_{\parallel} \delta B_r / B_0$, δJ_r is proportional to E_r . Surface charge continuity $\partial \sigma / \partial t = -\delta J_r$ will then give exponential decay of E_r because $\sigma \sim E_r$ through Poisson's equation $E_r = 4\pi\sigma / (1 + \omega_{pi}^2 / \Omega_{ci}^2) \approx 4\pi\sigma \Omega_{ci}^2 / \omega_{pi}^2$. The decay rate is

$$\gamma_m = \left(\frac{\delta B_r}{B_0} \right)^2 \frac{v_e l_m}{\rho_s^2}, \quad (3)$$

where ρ_s is the ion sound gyroradius. The decay rate goes as the perturbed magnetic field strength squared.

This estimate and the zero-beta tokamak calculations do not describe the impulsive response observed in gyrokinetic simulation with a radial magnetic field.⁵ In the latter all gradients and the magnetic shear are set to zero to remove instability dynamics. Starting from the standard $\beta = 0$ configuration, the zonal flow evolves from an initial state to a stable residual in the absence of collisions, with decaying oscillations due to geodesic acoustic modes. A radial magnetic field with a single resonant wavenumber is then introduced. The residual level evolves in response to the stochastic field perturbation. It does not asymptote to zero but varies approximately quadratically in time, passing

through zero in a finite time (see Fig. 4 of Ref. 5). The time to crossing varies inversely with the first power of the perturbed magnetic field strength.

Because this observed evolution differs so strongly from the prediction of simple theory or some stellarator results, both in form and in scaling a more careful calculation of the residual flow in the presence of magnetic flutter is needed. Agreement between the results of a careful theory and the observations would provide evidence that the non zonal transition is indeed caused by a disabling of zonal flows by the stochastic field.

In this paper we modify the calculation of Rosenbluth and Hinton^{8,9} to include a perturbed, externally imposed radial magnetic field. We treat the prompt charge loss from a rational surface due to the electrons, which for roughly comparable temperatures move much faster than ions. The electron response is calculated from the nonadiabatic gyrokinetic distribution with a magnetic flutter contribution included in the parallel operator. The electrons respond both to the initial charge and the time evolving potential. With both present the self-consistent evolution is complicated and can only be described in asymptotic limits. We assume that the response to flutter is faster than the curvature drift and neglect the latter. For ions we retain the Rosenbluth-Hinton response, consistent with the conditions in the numerical calculation at the time the perturbed radial field is turned on. We assume this response is valid until slower ion flutter losses start affecting the potential. Our calculation is for short times before the ion flutter response makes significant changes to the potential.

II. ION AND ELECTRON GYROKINETIC RESPONSES

A. Ions

The present calculation assumes ion physics in keeping with the treatment of Rosenbluth and Hinton for the residual flow. Accordingly we first review those results. The residual flow calculation treats the ion response to an impulsive charge (or potential) on a rational surface, assuming the electrons are adiabatic. The ion gyrokinetic equation is

$$\begin{aligned} \frac{\partial}{\partial t} f_{ki} + v_{\parallel} \hat{\mathbf{b}} \cdot \nabla f_{ki} + \omega_D f_{ki} + \frac{e}{T_i} F_0 J_0(k_{\perp} \rho_i) \\ \times [v_{\parallel} \hat{\mathbf{b}} \cdot \nabla + \omega_D] \Phi_k = S_k^{(i)}, \end{aligned} \quad (4)$$

where the symbols have the same meanings as in Refs. 8 and 9. The source $S_k^{(i)}$ is treated mathematically as a fixed impulsive ion charge proportional to a temporal delta function $\delta(t)$. In turbulence the charge results from nonlinear energy transfer, hence the impulse represents an instantaneous value of the nonlinearity of the formal gyrokinetic equation

$$S_k^{(i)} = - \sum_{k'} (\mathbf{k}' \times \hat{\mathbf{z}} \cdot \mathbf{k}) \left[\frac{c}{B_0} \Phi_k \right] J_0(k'_{\perp} \rho_i) J_0(k''_{\perp} \rho_i) f_{k'i}. \quad (5)$$

The potential Φ_k is determined from the quasineutrality condition, which takes the form

$$\int d^3 v f_{ke} + \frac{n_0 e \Phi_k}{T_i} = \int d^3 v J_0(k_{\perp} \rho_i) g_{ki}, \quad (6)$$

where f_{ke} is the electron distribution and g_{ki} is the nonadiabatic ion distribution given by

$$g_{ki} = \frac{e}{T_i} F_0 J_0(k_\perp \rho_i) \Phi_k + f_{ki}. \quad (7)$$

Expanding the Bessel function in the quasineutrality condition yields the form

$$\int d^3 v f_{ke} + e n_0 \left(\frac{k_\perp^2 \rho_i^2}{T_i} \right) \Phi_k = \int d^3 v f_{ki}. \quad (8)$$

In the Rosenbluth-Hinton calculation, the evolution of Eq. (4) is assumed to be dominated by $S_k^{(i)}$ and $\omega_D \Phi_k$. This is consistent with a solution for times long compared to the ion bounce time, for ion acoustic modes that are Landau damped, allowing for the neglect of $v_{\parallel} \hat{\mathbf{b}} \cdot \nabla f_{ki}$, and for $\beta = 0$, allowing $A_{\parallel k} = 0$. The equation is inverted in a drift kinetic ordering consistent with $J_0 \approx 1$ via an orbit integral over $S_k^{(i)} - (eF_0/T_i)\omega_D \Phi_k$, where an eikonal captures the rapid cross-field variation of Φ_k . The equations are bounce averaged with appropriate limits for both trapped and passing ions. Anticipating a time varying (impulsive) source, the Laplace transform is introduced, converting Eq. (8) to

$$n_0 \frac{e^2}{T_i} \chi_k(p) \hat{\Phi}(p) = \langle \tilde{\rho}_k^{(S)} \rangle, \quad (9)$$

where p is the Laplace transform variable and $\chi_k(p)$ is the plasma susceptibility, which contains bounce averages of the left hand side of Eq. (8) and the part of the right hand side proportional to the potential, and $\langle \tilde{\rho}_k^{(S)} \rangle$ is the charge density arising from the ion and electron sources

$$\langle \tilde{\rho}_k^{(S)} \rangle = \frac{e}{p} \left[\left\langle \int d^3 v S_k^{(i)} \right\rangle - \left\langle \int d^3 v S_k^{(e)} \right\rangle \right]. \quad (10)$$

The susceptibility accounts for ion orbits in the nonuniform magnetic field and is calculated to be^{8,9}

$$\chi_k(p) = k_\perp^2 \rho_i^2 \left(1 + 1.6 \frac{q^2}{\epsilon^{1/2}} \right). \quad (11)$$

With χ_k independent of p , the Laplace transform inversion is straightforward. As explained in Ref. 9, the solution to the initial value problem is given by the inverse transform of $k_\perp^2 \rho_i^2 / p \chi_k(p)$. Hence the temporal response of the potential to an impulsive charge density is given by

$$\frac{\Phi(t)}{\Phi(0)} = \frac{k_\perp^2 \rho_i^2}{2\pi i} \int \frac{dp e^{pt}}{p \chi_k(p)} = \frac{1}{1 + 1.6q^2/\epsilon^{1/2}}. \quad (12)$$

This susceptibility is the time-asymptotic response of the plasma to the impulse. Its dependencies on q and ϵ reflect the scaling of ion drifts in the inhomogeneous magnetic field.

B. Electrons

We now consider the electron dynamics and introduce a stochastic magnetic field. Electrons streaming along the

radial component move away from the rational surface. Their motion is faster than the ions; hence, there is a prompt electron loss. For times that are small relative to an ion streaming time along the radial field across a radial structure of scale k_x^{-1} the ions can be treated as not responding to the stochastic field. We consider a numerical experiment in which the potential is allowed to relax to the residual potential of Eq. (12) with $A_{\parallel k} = 0$. A stationary, externally imposed radial field $\tilde{B}_r = ik_y A_{\parallel k}$ is then switched on. This field has finite k_y ($k_y = 0.05$) and $k_x = 0$. We wish to determine how the $k_y = 0$ zonal potential evolves from that time onward under the loss of electrons due to the stochastic field.

This calculation, like the standard $\beta = 0$ problem,^{8,9} derives a test potential, not the self consistent potential that arises in turbulence above the NZT threshold. The potential is a test response because the nonlinearity is replaced with an impulsive source, as in Refs. 8 and 9, and because $A_{\parallel k}$ is fixed and not the self consistent vector potential of Ampere's law. The utility of this arrangement, both for the numerical experiment and the theoretical calculation, is to create a controlled situation where the physics is clear, as was performed in the original $\beta = 0$ calculation. In the latter, the potential is a linear response. In the present calculation, however, we now have the magnetic flutter term. In general, the flutter term is a magnetic nonlinearity with attendant complications. Here, with A_{\parallel} fixed, the flutter term is linear. In spite of this simplification, the spatial variation of A_{\parallel} interacts with the electron distribution through a convolution integral, i.e., through a linear mode-coupling process. The treatment of the mode coupling is detailed below.

For $t < B_0/\tilde{B}_0 k_x v_{thi}$ the $\beta = 0$ residual potential, which is the new initial condition for our calculation, continues to characterize the ion contribution to the potential. Potential evolution is governed entirely by the electron dynamics. In considering the removal of electrons from the vicinity of a rational (or drift) surface by streaming along a stochastic magnetic field, the flutter term $v_{\parallel} \nabla_{\parallel} = v_{\parallel} B_0^{-1} \tilde{B}_r \partial/\partial r = v_{\parallel} B_0^{-1} (\partial A_{\parallel}/\partial y)(\partial/\partial r)$ governs the dynamics and not the curvature drift and magnetic mirror terms important for motion confined to a drift surface. Consequently we simplify the electron response by neglecting the electron curvature drift and mirror terms.

The electron gyrokinetic equation then takes the form

$$\begin{aligned} \frac{\partial}{\partial t} f_k - v_{\parallel} \sum_{k'} \frac{k'_y}{B_0} A_{\parallel k'} (k_x - k'_x) f_{k-k'} \\ + \frac{eF_0}{T_e} v_{\parallel} \sum_{k'} \frac{k'_y}{B_0} A_{\parallel k'} (k_x - k'_x) \left[\Phi_{k-k'} - \frac{v_{\parallel}}{c} A_{\parallel k-k'} \right] = S_k^{(e)}, \end{aligned} \quad (13)$$

where the subscript e has been dropped in f_k and $S_k^{(e)}$ is the electron counterpart to $S_k^{(i)}$. For the numerical experiment that we are modeling $S_k^{(e)}$ defines the electron contribution to the charge at the time the radial magnetic field is turned on. Equation (13) is written in the general form appropriate when A_{\parallel} has a spectrum of wavenumbers. In the numerical calculation, there is only a single wavevector $\mathbf{k}' = (0.0, 0.05)$. Moreover, $\mathbf{k} = (0.05, 0.0)$ is a single

wavevector for the zonal response (in distribution function and potential). Consequently, the wavevector $\mathbf{k} - \mathbf{k}'$ represents a sideband fluctuation with a single wavevector. We will develop a representation of the mode coupling appropriate for these wavenumbers, but it is trivially generalized to an A_{\parallel} perturbation with multiple spectral components. We note that the third term in Eq. (13), which depends on the potentials, is sometimes neglected due to symmetry. The wavenumber configuration explained above eliminates the term proportional to $A_{\parallel k-k'}$. On the other hand, this configuration breaks any symmetry that would make $\Phi_{\parallel k-k'}$ vanish.

The sideband fluctuation is calculated by rewriting Eq. (13) for a fluctuation at $k - k'$, inverting the temporal operator, and substituting back into Eq. (13). Rewriting Eq. (13) for $k - k'$, the sideband distribution satisfies

$$\frac{\partial}{\partial t} f_{k-k'} = v_{\parallel} \sum_{k'} \frac{k_y''}{B_0} A_{\parallel k'}(k_x - k'_x - k_x'') f_{k-k'-k''} + \frac{eF_0}{T_e} v_{\parallel} \sum_{k'} \frac{k_y''}{B_0} A_{\parallel k'}(k_x - k'_x - k_x'') [\Phi_{k-k'-k''}]. \quad (14)$$

As above, the form is general, but the sideband interacts with the magnetic perturbation through the wavenumber k' of the magnetic perturbation, imposing $k'' = -k'$. Equation (14) is inverted by performing an orbit integral. In general, the interaction between k , k' , and $k - k'$ is subject to some form of decorrelation, which appears in a propagator associated with the orbit integral. Collisions produce decorrelation, but if the system is collisionless, the decorrelation must arise through other sideband couplings. We will represent the decorrelation with a diffusivity and find its form consistent with the flutter decrement $v_{\parallel} k_x k_y A_{\parallel} / B_0$, which is the only temporal rate in the problem. A self-consistent procedure for determining the form of the diffusivity consists of the following. A generic diffusion term is inserted into

$$\int_{t_0}^t dt' \exp[-D_{k-k'}(k_x - k'_x)^2(t-t')] f_k(t') \rightarrow \int_{t_0}^t \exp[-D_{k-k'}(k_x - k'_x)^2(t-t')] dt' f_k(t) = \frac{\exp[-D_{k-k'}(k_x - k'_x)^2(t-t')]}{-D_{k-k'}(k_x - k'_x)^2} \Big|_{t_0}^t f_k(t) \approx -\frac{f_k(t)}{D_{k-k'}(k_x - k'_x)^2}. \quad (17)$$

The last step requires that the initial time t_0 is far removed from the time t . When Eq. (17) is substituted into Eq. (16), we obtain

$$\frac{\partial}{\partial t} f_k + v_{\parallel}^2 \sum_{k'} \frac{k_y^2}{B_0^2} \frac{A_{\parallel k'} A_{\parallel -k'}(k_x - k'_x) k_x}{D_{k-k'}(k_x - k'_x)^2} \left[f_k(t) - \frac{eF_0}{T_e} \Phi_k(t) \right] + \frac{eF_0}{T_e} v_{\parallel} \sum_{k'} \frac{k_y'}{B_0} A_{\parallel k'}(k_x - k'_x) \Phi_{k-k'} = S_k^{(e)}. \quad (18)$$

The second term (proportional to f_k) is a diffusivity that depends on the magnitude of the magnetic perturbation. Equating it to the original form $D_k k_x^2$ gives the form of the diffusivity consistent with decorrelation by flutter

the problem, i.e., $\partial_t f_{k-k'} \rightarrow [\partial_t + D_{k-k'}(k_x - k'_x)^2] f_{k-k'}$. The substitution of the inversion of Eq. (14) into Eq. (13) reveals the form of the diffusivity from a coherent damping term that depends on the perturbation amplitude A_{\parallel} (i.e., an A_{\parallel} -dependent term proportional to f_k). These steps are mathematically identical to those of closure theory,¹³ specifically closure theory that assumes that interactions are subject to decorrelation caused by an amplitude-dependent (eddy) damping process.¹⁴

Performing the formal inversion of Eq. (14)

$$f_{k-k'}(t) = \int_{t_0}^t dt' \exp[-D_{k-k'}(k_x - k'_x)^2(t-t')] \times \left[v_{\parallel} \frac{k_y' k_x}{B_0} A_{\parallel -k'} \left(f_k(t') - \frac{eF_0}{T_e} \Phi_k(t') \right) \right]. \quad (15)$$

Substituting Eq. (15) into Eq. (13) yields

$$\frac{\partial}{\partial t} f_k - v_{\parallel}^2 \sum_{k'} \int_{t_0}^t dt' \exp[-D_{k-k'}(k_x - k'_x)^2(t-t')] \times \frac{k_y^2}{B_0^2} A_{\parallel k'} A_{\parallel -k'}(k_x - k'_x) k_x \left(f_k(t') - \frac{eF_0}{T_e} \Phi_k(t') \right) + \frac{eF_0}{T_e} v_{\parallel} \sum_{k'} \frac{k_y'}{B_0} A_{\parallel k'}(k_x - k'_x) \Phi_{k-k'} = S_k^{(e)}. \quad (16)$$

The term proportional to $f_k(t')$ represents a damping process that depends on the magnitude of the magnetic perturbation. It does not quite have the form $D_k k_x^2 f_k$ because of the temporal convolution associated with the time history integral. When the integral is subjected to a Markovian assumption, the desired form is obtained. The Markovian treatment of the time history integral assumes that f_k evolves on a slower time scale than $(D_k k^2)^{-1}$ so that

$$D_k = v_{\parallel}^2 \sum_{k'} \frac{k_y^2}{B_0^2} \frac{A_{\parallel k'} A_{\parallel -k'}(1 - k'_x/k_x)}{[D_{k-k'}(k_x - k'_x)^2]}. \quad (19)$$

Equation (19) is general. To reduce it to the form consistent with the numerical calculation we take $k'_x = 0$ and k'_y a single wavenumber, yielding

$$D_k k_x^2 = \frac{v_{\parallel}^2 k_y^2 |A_{\parallel k'}|^2}{B_0^2}. \quad (20)$$

With Eq. (20), magnetic flutter is represented as a diffusivity process. The diffusivity has the simplest form consistent with physical dimensions and corresponds to the type of

renormalization of temporal response obtained in nonlinear closure calculations.^{13,14} Closure calculations assume many interactions, each of which is weak, and this assumption is consistent with the notion of weak sideband coupling in the present calculation. For weak coupling it is also standard to neglect the renormalization of the potential [dropping the last term on the left hand side of Eq. (18)]. Dropping this term and substituting the weak-coupling form of D , the electron equation becomes

$$\frac{\partial}{\partial t} f_k + v_{\parallel} \frac{k'_y}{B_0} A_{\parallel k'} k_x f_k - \frac{eF_0}{T_e} v_{\parallel} \frac{k'_y}{B_0} A_{\parallel k'} k_x \Phi_k = S_k^{(e)}. \quad (21)$$

The approximations made in deriving Eq. (21) are marginally satisfied for the numerical experiment we seek to understand. This is particularly true for the Markovian assumption, whose time scale separation puts it in a gray area between validity and breakdown. However, the approximations enable a calculation of the zonal potential in a form that is amenable to comparison with simulation. It makes sense to perform the comparison and test how well the diffusive representation models the potential response in the presence of flutter. Importantly, the scalings of Eq. (21) preserve the scalings of the flutter. Hence, regardless of the approximations made, the scalings of the calculation and an exact solution will be the same. Accordingly, comparisons with the scalings of the numerical experiment will provide a test of whether flutter is the source of the numerical behavior.

As an aside, we note that the electron equation and flutter nonlinearity have the same form given in Eq. (21) in another limit. If the magnetic perturbation is large-scale or dominated by large scales relative to k , then $k' \gg k$ and Eq. (13) immediately reduces to Eq. (21).

It is straightforward to invert Eq. (21) with a temporal Green function. The result is

$$f_{ke} = \exp \left[-v_{\parallel} k_x k'_y \frac{A_{\parallel k'}}{B_0} t \right] \int_0^t dt' \exp \left[v_{\parallel} k_x k'_y \frac{A_{\parallel k'}}{B_0} t' \right] \times \left[S_k^{(e)} + v_{\parallel} k_x k'_y \frac{A_{\parallel k'}}{B_0} \frac{eF_0}{T_e} \Phi_k \right]. \quad (22)$$

We note that if $S_k^{(e)} = 0$ and Φ_k is constant, we recover an adiabatic response $f_{ke} = (eF_0/T_e)\Phi_k$. If $S_k^{(e)} = f_{ke}(0)\delta(t')$ and $\Phi_k = 0$, f_{ke} decays exponentially at the flutter streaming rate. When Φ_k evolves self consistently via the quasineutrality condition it is a function of time. Its variation is then convolved with the exponential streaming factors, which constitute the Green function.

III. POTENTIAL EVOLUTION

Combining ion and electron responses, the quasineutrality condition becomes

$$\begin{aligned} & \frac{n_0 e}{T_i} k_{\perp}^2 \rho_i^2 \left(1 + 1.6 \frac{q^2}{\epsilon^{1/2}} \right) \Phi_k(t) \\ &= \int d^3 v S_k^{(i)} - \int d^3 v \tilde{S}_k^{(e)} \exp \left[-v_{\parallel} k_x k'_y \frac{A_{\parallel k'}}{B_0} t \right] \\ & \quad - \int d^3 v v_{\parallel} k_x k'_y \frac{A_{\parallel k'}}{B_0} \frac{eF_0}{T_e} \int_0^t dt' \Phi_k(t') \\ & \quad \times \exp \left[-v_{\parallel} k_x k'_y \frac{A_{\parallel k'}}{B_0} (t - t') \right], \end{aligned} \quad (23)$$

where $\tilde{S}_k^{(e)}$ is the amplitude of the electron impulse, $S_k^{(e)} = \tilde{S}_k^{(e)} \delta(t)$. With $A_{\parallel k'}$ stationary this is an integral equation for Φ_k . When $A_{\parallel k'}$ evolves self consistently, inclusion of Ampere's law yields two coupled integral equations for $\Phi_k(t)$ and $A_{\parallel k}(t)$. This problem will be addressed elsewhere. We perform the integral over v_{\parallel} , assuming that the electron source has a Maxwellian velocity distribution $\hat{S}_k^{(e)} = \bar{S}_k^{(e)} F_0(v) = \bar{S}_k^{(e)} F_{\parallel}(v_{\parallel}) F_{\perp}(v_{\perp})$, where F_{\parallel} and F_{\perp} are normalized Maxwellian distributions for v_{\parallel} and v_{\perp} . In Sec. V, where comparisons with numerical simulations are undertaken, the v_{\parallel} -integrated electron source $\bar{S}_k^{(e)}$ is equivalent to the perturbed electron density at $t=0$. Integration over a Maxwellian in v_{\parallel} makes the exponential functions of time Maxwellian functions of time, yielding

$$\begin{aligned} & \frac{n_0 e}{T_i} k_{\perp}^2 \rho_i^2 \left[\left(1 + 1.6 \frac{q^2}{\epsilon^{1/2}} \right) \Phi_k(t) - \Phi_k(0) \right] \\ &= -2 \int d^2 v_{\perp} F_{\perp}(v_{\perp}) \bar{S}_k^{(e)} \left[\exp \left(v_e^2 k_x^2 k_y^2 \frac{A_{\parallel k'}^2}{B_0^2} t^2 \right) - 1 \right] \\ & \quad - 4n_0 v_e^2 k_x^2 k_y^2 \frac{A_{\parallel k'}^2}{B_0^2} \int_0^t dt' (t - t') \frac{e\Phi_k(t')}{T_e} \\ & \quad \times \exp \left[v_e^2 k_x^2 k_y^2 \frac{A_{\parallel k'}^2}{B_0^2} (t - t')^2 \right], \end{aligned} \quad (24)$$

where ion and electron source terms have been folded into the initial potential $\Phi_k(0)$ and v_e is the electron thermal velocity.

This is an integral equation for $\Phi_k(t)$ that involves a convolution of $\Phi_k(t)$. A Laplace transform $\hat{\Phi}(p) = \int_0^{\infty} \Phi_k(t) \exp(-pt) dt$ of the equation deconvolves the convolution integral and allows the Laplace transform potential $\hat{\Phi}(p)$ to be written as a function of the other temporal dependencies of Eq. (24). The result is

$$\hat{\Phi}(p) = \left[\frac{\Phi(0)}{pR} + 2 \left(\frac{n_0 e}{T_i} k_{\perp}^2 \rho_i^2 R \right)^{-1} \int d^2 v_{\perp} F_{\perp}(v_{\perp}) \bar{S}_k^{(e)} I(p) \right] \left[1 - \frac{T_i}{T_e} \left(\pm \frac{2p}{\alpha} \right) \frac{I_{\pm}(p)}{k_{\perp}^2 \rho_i^2 R} \right]^{-1}, \quad (25)$$

where

$$I_{\pm}(p) = \left[\frac{i\sqrt{\pi}}{2\alpha} \exp \left(-\frac{p^2}{4\alpha^2} \right) \operatorname{erfc} \left(\mp \frac{ip}{2\alpha} \right) \pm \frac{1}{p} \right], \quad (26)$$

$$\alpha = v_e k_x k'_y \frac{A_{||k'}}{B_0}, \quad (27)$$

and

$$R = 1 + 1.6 \frac{q^2}{\epsilon^{1/2}} \quad (28)$$

is the residual factor of Rosenbluth and Hinton. There are two branches in Eqs. (25) and (26) arising from a transformation $\tau = \pm(t - p/2\alpha^2)$ introduced to do the Laplace transform integral $\int_0^\infty dt \exp(\alpha^2 t^2 - pt)$. The transform of Eq. (25) back to the temporal domain creates a convolution of the two factors in square brackets, yielding

$$\Phi_k(t) = \int_0^t \lambda(t') \kappa(t - t') dt', \quad (29)$$

where

$$\lambda(t) = \frac{\Phi(0)}{R} - 2 \left(\frac{n_0 e}{T_i} k_\perp^2 \rho_i^2 R \right)^{-1} \int d^2 v_\perp F_\perp(v_\perp) \bar{S}_k^{(e)} [\exp(\alpha^2 t^2) - 1] \quad (30)$$

and

$$\kappa(t) = \frac{1}{2\pi i} \int_{-i\infty+p_0}^{i\infty+p_0} dp \exp(pt) \left[1 - \frac{2T_i p I_\pm(p)}{T_e k_\perp^2 \rho_i^2 R} \right]^{-1}. \quad (31)$$

With the function $I(p)$ in the denominator of the inverse Laplace transform given by Eq. (31), $\kappa(t)$ is not available from the Laplace transform operations previously performed in this calculation. Consequently other means for solving the equation must be found. If $\kappa(t)$ is found from an approximation or expansion, it is important to maintain the proper initial-value content of the Laplace transform solution. As

the problem has been formulated, the initial condition is $\Phi(t=0) = \Phi(0)/R$. We note that $\lim_{t \rightarrow 0} \lambda(t) = \Phi(0)/R$, because the second term on the rhs of Eq. (30) goes as $\alpha^2 t^2$ for small t . Consequently, $\kappa(t)$ must satisfy

$$\lim_{t \rightarrow 0} \kappa(t) = \delta(t). \quad (32)$$

While Eqs. (29)–(31) are the solution of the time-dependent potential in the presence of magnetic flutter, their form is too complicated for immediate comparison with the results of simulation.⁵ For comparison with numerical results we evaluate the integral of Eq. (31).

IV. SOLUTION OF RESIDUAL FLOW RESPONSE

As an inverse Laplace transform, Eq. (31) could be evaluated by contour methods that account for the poles of the integrand. There are an infinite number of poles, corresponding to zeros of

$$Z_\pm(p) = \left[1 - \frac{2T_i p I_\pm(p)}{T_e k_\perp^2 \rho_i^2 R} \right]. \quad (33)$$

Figure 1 shows contours of $\text{Re}Z_+(p) = 0$ and $\text{Im}Z_+(p) = 0$ for $C_0 = T_i/(T_e k_\perp^2 \rho_i^2 R) = 10$. Zeros of $Z_+(p)$ correspond to the points where the curves cross. We observe that there are poles for both positive and negative values of $\text{Re}p$, and that the pole spacing becomes narrower as $\text{Re}p$ and $\text{Im}p$ increase. The latter feature leads to the conclusion that the series generated by summing over residues is not converged. Moreover, the resulting form is not transparent with regard to the initial value problem. Consequently we do not attempt to integrate Eq. (31) by contour methods.

Instead we seek an expansion for small time, which corresponds to the temporal domain of Fig. 4 of Ref. 5. The expansion parameter for small t is $\alpha t \ll 1$. An appropriate expansion can be developed by writing $\kappa(t)$ as

$$\begin{aligned} \kappa(t) &= \frac{1}{2\pi i} \int_{-i\infty+p_0}^{i\infty+p_0} dp \exp(pt) \left[1 + \frac{2T_i p I_\pm(p)}{T_e k_\perp^2 \rho_i^2 R} \left(1 - \frac{2T_i p I_\pm(p)}{T_e k_\perp^2 \rho_i^2 R} \right)^{-1} \right], \\ &= \delta(t) + \frac{1}{2\pi i} \int_{-i\infty+p_0}^{i\infty+p_0} dp \exp(pt) \left[\frac{2T_i p I_\pm(p)}{T_e k_\perp^2 \rho_i^2 R} \left(1 - \frac{2T_i p I_\pm(p)}{T_e k_\perp^2 \rho_i^2 R} \right)^{-1} \right]. \end{aligned} \quad (34)$$

Writing $I_\pm(p)$ explicitly

$$\kappa(t) = \delta(t) + \frac{1}{2\pi i} \int_{-i\infty+p_0}^{i\infty+p_0} dp \exp(pt) \frac{(T_i/T_e) \left[2 \pm i \left(\frac{\sqrt{\pi}}{\alpha} \right) p \exp(-p^2/4\alpha^2) \text{erfc} \left(\pm \frac{ip}{2\alpha} \right) \right]}{k_\perp^2 \rho_i^2 R - (2T_i/T_e) \mp i \left(\frac{\sqrt{\pi}}{\alpha} \right) p \exp(-p^2/4\alpha^2) \text{erfc} \left(\pm \frac{ip}{2\alpha} \right)}. \quad (35)$$

The limit $\alpha t \ll 1$ corresponds to $p/\alpha \gg 1$, allowing the demoninator to be expanded as

$$\left[k_{\perp}^2 \rho_i^2 R - \frac{2T_i}{T_e} \mp i \sqrt{\pi} \left(\frac{p}{\alpha} \right) \exp\left(-\frac{p^2}{4\alpha^2}\right) \operatorname{erfc}\left(\pm \frac{ip}{2\alpha}\right) \right]^{-1} \\ = \frac{1}{k_{\perp}^2 \rho_i^2 R - (2T_i/T_e)} \left\{ 1 + \sum_{n=1}^{\infty} \left[\frac{\mp i (\sqrt{\pi} p / \alpha) \exp(-p^2/4\alpha^2) \operatorname{erfc}(\pm ip/2\alpha)}{k_{\perp}^2 \rho_i^2 R - (2T_i/T_e)} \right]^n \right\}. \quad (36)$$

The lowest order contribution to the integral in Eq. (35) is readily evaluated, yielding

$$\kappa(t) = \delta(t) + \frac{2\alpha^2 t \exp(\alpha^2 t^2)}{1 - k_{\perp}^2 \rho_i^2 R T_e / 2T_i} + O(\alpha^3 t^2). \quad (37)$$

We note that this form satisfies the initial value constraint on κ given by Eq. (32).

With this expression and Eq. (30) we integrate Eq. (29) to obtain

$$\Phi(t) = \frac{\Phi(0)}{R} \left[1 + \frac{\exp(\alpha^2 t^2) - 1}{1 - k_{\perp}^2 \rho_i^2 R T_e / 2T_i} \right] \\ - \frac{2}{(n_0 e / T_i) k_{\perp}^2 \rho_i^2 R} \int d^2 v_{\perp} F_0(v_{\perp}) \bar{S}_k^{(e)} \\ \times [\exp(\alpha^2 t^2) - 1] + O(\alpha^4 t^4). \quad (38)$$

This expression holds for both branches introduced in Eq. (25). A consistent expansion, in which only those terms that are order $\alpha^2 t^2$ and smaller are retained, is given by

$$\Phi(t) = \frac{\Phi(0)}{R} \left[1 + \frac{\alpha^2 t^2}{1 - k_{\perp}^2 \rho_i^2 R T_e / 2T_i} \right] \\ - \frac{2}{(n_0 e / T_i) k_{\perp}^2 \rho_i^2 R} \int d^2 v_{\perp} F_0(v_{\perp}) \bar{S}_k^{(e)} \alpha^2 t^2. \quad (39)$$

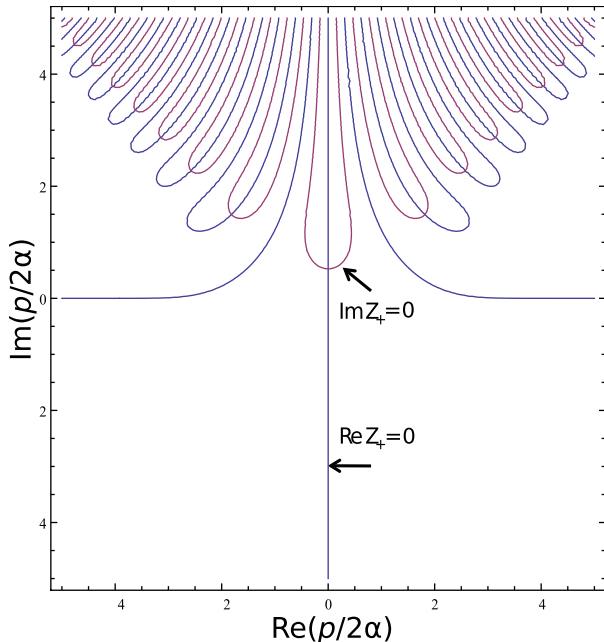


FIG. 1. Contours of $\operatorname{Re} Z_{\pm}(p) = 0$ (blue) and $\operatorname{Im} Z_{\pm}(p) = 0$ (red) for $C_0 = T_i / (T_e k_{\perp}^2 \rho_i^2 R) = 10$. The zeros correspond to the points where contours cross.

This expression is quadratic in time and will be compared with the simulation results in Sec. V.

V. COMPARISON WITH SIMULATIONS

Having derived an analytical expression in Eq. (39) that describes the flutter effect on the residual potential for moderately short times t , we now compare this result with numerical simulations. To this end, the *GENE* code,^{15,16} an electromagnetic gyrokinetic Vlasov solver, is used in its radially local mode of operation, with \hat{s} - α geometry,¹⁷ and switching off compressional magnetic fluctuations. After a few words on the simulation setup, we compare numerical parameter dependencies with those of the theory, as well as the absolute magnitude of the effect.

An initialized zonal flow decays, in the absence of magnetic fluctuations, to its residual; at that point in time t_R , an artificially imposed B_x , which is constant in time and along the background magnetic field, is switched on at $k_x = 0$, leading to a “decay” of the residual, as is to be expected from the above considerations. Note that with this setup, B_x is flux-surface-breaking whereas no effect is observed when flux-surface-preserving fluctuations are added.

The characteristic time scale for the decay depends on the physical input parameters, as well as on the initial setting for n_e / Φ . As described in more detail in Ref. 18, one may initialize either the zonal flow in Φ directly (hereafter IC1) or by setting the densities (hereafter IC2), with a different resulting n_e / Φ . The latter method leads to somewhat different dynamics before the system settles in the residual state, but it allows for significant reduction in simulation cost. We stress that both approaches are compatible with the decay dynamics of Eq. (39). Also, note that for simulations with adiabatic electrons, IC1 and IC2 are identical—for the present work, however, the use of explicit computation of the electrons is essential.

In the following, we use IC2 unless specified otherwise. Further details on numerical resolutions and (collisional and/or hyperdiffusive) dissipation can be found in Ref. 18. It suffices to say here that these simulations were thoroughly tested for convergence. First, we compare the scaling of the time $t_{\Phi=0}$ with essential physical parameters for both simulations and theory. The point in time $t_{\Phi=0}$ is defined as the moment when Φ changes sign. As this tends to occur at reasonably short times, it is assumed that the quadratic expansion $\Phi - \Phi_0 / R \propto -\alpha^2 t^2$ holds. Note that $t_{\Phi=0}$ is offset by t_R , the time at which the magnetic perturbation is switched on. Typical values of $\alpha t_{\Phi=0}$ are in the neighborhood of 0.2 for turbulence relevant parameters, as shown in Ref. 18.

Figures 2–4 show the scaling of $t_{\Phi=0}$ with the magnetic perturbation amplitude A_{\parallel} , the ion temperature T_i , and the

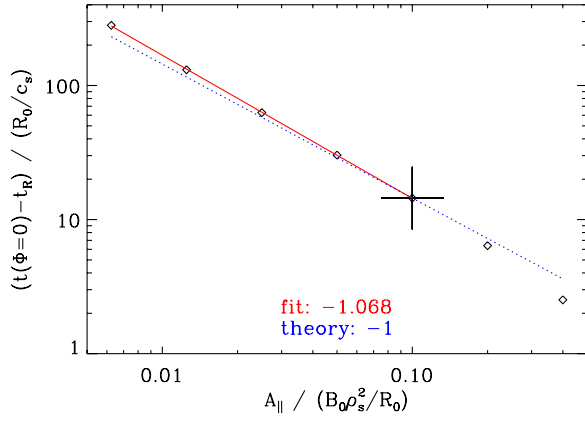


FIG. 2. Zero crossing time of Φ as a function of the magnetic perturbation level. A fit is shown as a solid red line which compares well with the analytical slope (blue dotted line).

safety factor q_0 , respectively. Only one parameter is varied at a time, with the following Cyclone-like default set (marked by a large cross in each plot): $k_{(x,y)}\rho_s = (0.05, 0.05)$, $T_i = T_e$, $q_0 = 1.4$, $\epsilon_t = 0.18$, and $A_{\parallel} = 0.1$. This constitutes a low- k limit where the last term in Eq. (39) can be expected to dominate the decay. Clearly, the predicted slopes match the numerical results quite well, as indicated by the fit values.

One feature common to the data on which these plots are based is that as the parameters are changed, both the oscillatory behavior at $t < t_R$ and the validity of the quadratic expansion at $t_{\Phi=0}$ are affected, if only slightly. While this causes small deviations from the theoretical predictions, the overall effect is small for the aforementioned parameter scalings.

This is no longer the case, however, when scanning over the inverse aspect ratio ϵ_t of the flux surface under consideration. For this case, a number of issues—from the large-aspect-ratio limit breaking down to large values of the residual factor R —pollute the results, making a more careful analysis necessary. We therefore analyze a different set of simulations, this time with the more expensive initial condition IC1. One difference lies in a cleaner onset of the decay, resulting in better measurements of $t_{\Phi=0}$ (see the diamonds and the red fit curve in Fig. 5). In the experimentally relevant

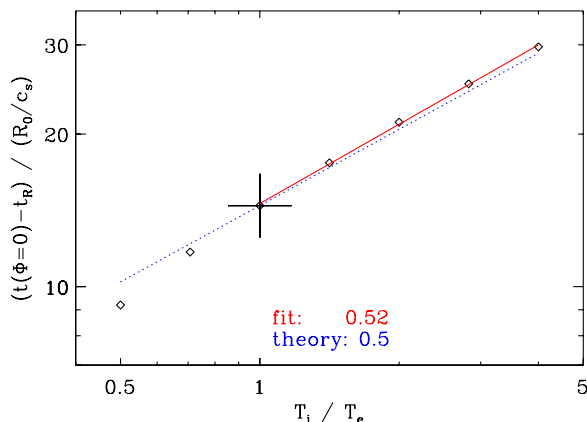


FIG. 3. Zero crossing time of Φ as a function of the ion temperature. A fit is shown as a solid red line which compares well with the analytical slope (blue dotted line).

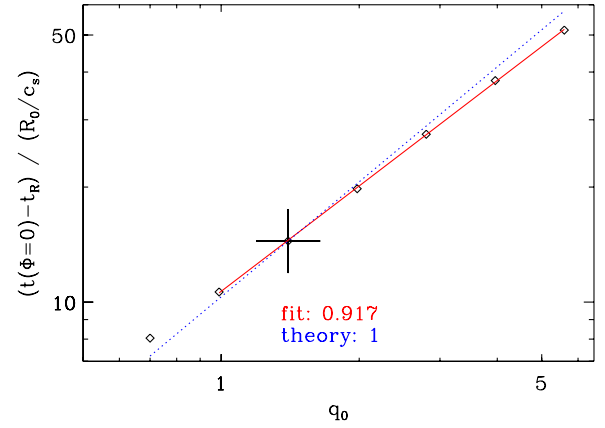


FIG. 4. Zero crossing time of Φ as a function of the safety factor. A fit is shown as a solid red line which compares well with the analytical slope (blue dotted line).

range $0.08 \leq \epsilon_t \leq 0.3$, one observes reasonably good agreement. Further enhancing the comparison with the theoretical predictions, instead of measuring $t_{\Phi=0}$ explicitly, we fit a parabola to the decaying $\Phi(t)$ curve at short times and take the zero of that parabola as the zero crossing time of Φ . The result, marked by x's and the dashed purple fit curve in Fig. 5, demonstrates that good agreement with the theory is achieved over a significant range of ϵ_t values.

Having shown the applicability of Eq. (39) where its main parameter dependencies are concerned, we now turn to how well it describes the absolute magnitude of the magnetic-perturbation-induced decay of Φ . To this end, we focus on the default parameter set common to Figs. 2–4.

Equation (39), for the purpose of comparing with the simulations, reduces to

$$\frac{\Phi}{\Phi(t'=0)/R} = 1 - \frac{n_e(t'=0)/\Phi(t'=0)}{k_x^2 R} \alpha^2 t^2, \quad (40)$$

where we have normalized k_x to ρ_s (the ion sound gyroradius), Φ to $T_e \rho_s / (eR_0)$, and n_e to $n_0 \rho_s / R_0$. Moreover, with the electron thermal velocity as the parallel streaming

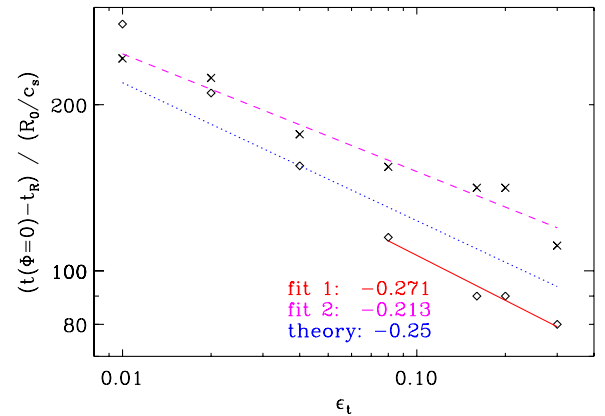


FIG. 5. Zero crossing time of Φ as a function of the inverse aspect ratio. Numerical results were obtained for IC1, resulting in improved agreement of the numerical results (black diamonds, fitted by the red solid line) with the analytical slope (blue dotted line). Using parabolic fits to determine $t_{\Phi=0}$ yields good agreement over a larger range (black crosses, purple dashed line).

velocity, $\alpha^2 = (m_i/m_e)k_x^2(B_x^2/B_0^2)$, with B_x normalized to $B_0\rho_s/R_0$. Note that $t=0$ now marks the point when the magnetic fluctuations are turned on, whereas $t'=0$ denotes the beginning of the simulation. Setting $\Phi=0$, one obtains

$$t_{\Phi=0} = \frac{R\Phi(t'=0)/n_e(t'=0)}{(m_i/m_e)(B_x/B_0)}. \quad (41)$$

With $\Phi(t'=0)/n_e(t'=0) = 0.499$ measured in the simulations, we thus obtain $t_{\Phi=0} = 19.56$. Now, recall that we used $v_{\parallel} = v_{\text{th},e} = (T_e/m_e)^{1/2}$ as the parallel velocity. However, in GENE, the parallel velocity space is normalized to $v_{\text{Th},e} = (2T_e/m_e)^{1/2}$. Taking this latter definition, α is increased by a factor of $2^{1/2}$, and $t_{\Phi=0}$ lowered to 13.8. This compares very well with the numerical value of 14.5 although we would like to stress that there is some freedom in selecting the exact value for the parallel velocity, and that $\pm 30\%$ may therefore be a better estimate for the accuracy of the theoretical expressions.

Based on both this finding and the above good agreement of the parameter dependencies, we conclude that our analytical theory, and in particular Eq. (39), provide a reasonable description of the physics underlying the phenomenon of residual flow decay in the presence of flux-surface-breaking magnetic fluctuations.

VI. CONCLUSIONS

This paper has described a generalization of the residual flow calculation of Rosenbluth and Hinton^{8,9} to include the effect of an externally imposed radial magnetic field perturbation in a tokamak equilibrium. The generalization involves the calculation of the nonadiabatic electron response to the impulsive charge perturbation that sets the initial state in relaxation to the residual flow. Our primary interest is the charge loss from otherwise closed orbits caused by electron streaming along the radial field component; hence, the electron dynamics is assumed to be dominated by magnetic flutter. For a simple radial magnetic field perturbation involving a single wavenumber and weak coupling with sideband fluctuations, the magnetic flutter term assumes a simple form and allows analytic solution of the potential for the short times over which ion flutter losses can be neglected relative to those of electrons.

When the magnetic perturbation is switched on once the potential has relaxed to the $\beta=0$ residual, the potential varies quadratically in time for short times, going through zero after a finite time. This behavior is observed in simulations with the same configuration, but was not anticipated from a simple tokamak calculations presented in the introduction or from some residual flow calculations for stellarators.^{10,11} These latter calculations yield exponential decay, and the time constant in the simple tokamak calculation goes like the square of the magnetic field perturbation. The linear scaling with perturbed magnetic field strength predicted by the theory agrees well with the scaling of the simulation result. So too do scalings with ion temperature, safety factor, and aspect ratio. These comparisons confirm that the potential variation in the numerical residual flow experiments⁵ is

caused by the charge loss from rational surfaces due to magnetic flutter.

Certain residual-flow studies for stellarators have yielded low-frequency oscillatory behavior¹² that may have some connection for early times to the results described here with a zero crossing for the potential. There is obviously similarity between the stationary, externally imposed radial magnetic field of this paper and 3D stellarator geometry where the non-axisymmetric part of the magnetic field is also stationary and externally imposed. However, as the present calculation assumes an axisymmetric equilibrium, it makes no explicit accounting for 3D non ambipolar losses and the radial electric fields they set up. Therefore the question of how these results might relate to stellarators would benefit from further investigation.

The calculation described here does not describe the potential arising from motion along a stochastic field in turbulent situations where charge distributions on flux surfaces are time dependent and self consistently driven by nonlinearity, and the magnetic field perturbations are self consistently governed by Ampere's law. Rather, the special impulsive response calculated in this theory is designed to match the numerical residual-flow experiment described in Sec. V and thus ascertain which physical processes govern the potential in the presence of a radial magnetic field perturbation. Together, the theory and experiment support an explanation for the non zonal transition in ITG turbulence, where very large transport levels are seen above a critical threshold in β . This explanation attributes the high transport levels to a disabling of zonal flows by charge loss associated with particle streaming along stochastic fields at finite β . As noted in Ref. 18, this explanation is further bolstered by a comparison of the turbulent correlation time and the time to disable zonal flows ($\sim t_{\Phi=0}$), which shows them to be comparable. With zonal flows eliminated, transport rates are higher regardless of the whether the mechanism by which zonal flows affect transport is shearing, or as recently demonstrated, is due to enhanced transfer to damped modes.^{19,20}

ACKNOWLEDGMENTS

The authors acknowledge useful conversations with Frank Jenko, Chris Hegna, and Felix Parra. This work was supported by US Department of Energy (Grant No. DE-FG02-89ER53291) and the Center for Momentum Transport and Flow Organization.

¹M. J. Pueschel and F. Jenko, *Phys. Plasmas* **17**, 062307 (2010).

²R. E. Waltz, *Phys. Plasmas* **17**, 072501 (2010).

³A. Dimits, G. Bateman, M. A. Beer, B. I. Cohen, W. Dorland, G. W. Hammett, C. Kim, J. E. Kinsey, M. Kotschenreuther, A. H. Kritz, L. L. Lao, J. Madrekas, W. M. Nevins, S. E. Parker, A. J. Redd, D. E. Shumaker, R. Sydora, and J. Weiland, *Phys. Plasmas* **7**, 969 (2000).

⁴W. M. Nevins, E. Wang, I. Joseph, J. Candy, S. E. Parker, Y. Chen, and G. Rewoldt, <http://meetings.aps.org/link/BAPS.2009.DPP.BP8.18>.

⁵M. J. Pueschel, P. W. Terry, F. Jenko, D. R. Hatch, T. Gorler, W. M. Nevins, and D. Told, *Phys. Rev. Lett.* **110**, 155005 (2013).

⁶D. R. Hatch, M. J. Pueschel, W. M. Nevins, F. Jenko, P. W. Terry, and H. Doerk, *Phys. Rev. Lett.* **108**, 235002 (2012).

⁷D. R. Hatch, M. J. Pueschel, F. Jenko, W. M. Nevins, P. W. Terry, and H. Doerk, *Phys. Plasmas* **20**, 012307 (2013).

- ⁸M. N. Rosenbluth and F. L. Hinton, *Phys. Rev. Lett.* **80**, 724 (1998).
- ⁹F. L. Hinton and M. N. Rosenbluth, *Plasma Phys. Controlled Fusion* **41**, A653 (1999).
- ¹⁰H. Sugama and T.-H. Watanabe, *Phys. Plasmas* **13**, 012501 (2006).
- ¹¹P. Helander, A. Mishchenko, R. Kleiber, and P. Xanthopoulos, *Plasma Phys. Controlled Fusion* **53**, 054006 (2011).
- ¹²P. Xanthopoulos, A. Mischchenko, P. Helander, H. Sugama, and T.-H. Watanabe, *Phys. Rev. Lett.* **107**, 245002 (2011).
- ¹³R. H. Kraichnan, *J. Fluid Mech.* **5**, 497 (1959).
- ¹⁴S. A. Orszag, *J. Fluid Mech.* **41**, 363 (1970).
- ¹⁵F. Jenko, W. Dorland, M. Kotschenreuther, and B. N. Rogers, *Phys. Plasmas* **7**, 1904 (2000).
- ¹⁶See <http://gene.rzg.mpg.de> for code details and access.
- ¹⁷J. Connor, R. Hastie, and J. Taylor, *Phys. Rev. Lett.* **40**, 396 (1978).
- ¹⁸M. J. Pueschel, D. R. Hatch, T. Görler, W. M. Nevins, F. Jenko, P. W. Terry, and D. Told, *Phys. Plasmas* **20**, 102301 (2013).
- ¹⁹K. Makwana, P. W. Terry, and J.-H. Kim, *Phys. Plasmas* **19**, 062310 (2012).
- ²⁰K. Makwana, P. W. Terry, M. J. Pueschel, and D. R. Hatch, "Subdominant modes in zonal-flow-regulated turbulence," *Phys. Rev. Lett.* (submitted).